Nonseparable Werner states in spontaneous parametric down-conversion

Marco Caminati,[1] Francesco De Martini,[1] Riccardo Perris,[1] Fabio Sciarrino,[2,1] and Veronica Secondi[1]

[1]*Dipartimento di Fisica, Università "La Sapienza," Roma 00185, Italy*

[2]*Centro di Studi e Ricerche "Enrico Fermi," Via Panisperna 89/A, Compendio del Viminale, Roma 00184, Italy*

The multiphoton states generated by high-gain spontaneous parametric down-conversion (SPDC) in the presence of large losses are investigated theoretically and experimentally. The explicit form for the two-photon output state has been found to exhibit a Werner structure very resilient to losses for any value of the nonlinear gain parameter g. The theoretical results are found to be in agreement with experimental data obtained by "entanglement witness" methods and by the quantum tomography of the state generated by a high-g SPDC.

I. INTRODUCTION

Entanglement, the nonclassical correlation between distant quantum systems, represents a physical resource lying at the foundations of quantum information (QI), quantum computation, and quantum communication. The current proliferation of relevant applications of quantum entanglement, ranging from one-way quantum computation [1] to the emerging fields of quantum metrology, lithography, etc. [2], strengthens the need for new flexible and reliable techniques to generate entangled states with increasing dimensions.

Entangled photonic qubit pairs generated under suitable phase-matching conditions by spontaneous parametric down-conversion (SPDC) in a nonlinear (NL) crystal have been central to many applications ranging from teleportation [3] to various quantum key distribution protocols [4]. Today the realization of reliable SPDC sources with large efficiency, i.e., with large "brilliance," able to generate entangled pure states is of key interest as they largely determine the range of applications of the sophisticated optical methods required by modern QI. Recently, high-brilliance sources of polarization-entangled states have been realized by using bulk crystals [5–7], periodically poled NL crystals [8], and bulk crystals with fiber-coupled SPDC radiation [9]. The extension of these methods to higher-dimensional QI qubit spaces could lead to new information processing tasks [10] and requires the development of appropriate technological and theoretical tools.

In this framework the investigation of multiphoton states is of fundamental importance, on both conceptual and practical levels, e.g., for nonlocality tests [11,12] or for QI applications [10]. The direct approach to generating bipartite multiphoton entanglement is the adoption of the SPDC process in a high-gain (HG) regime. The number of photons generated depends on the nonlinear gain g of the parametric process; g can be increased by the adoption of a high-power pumping laser and high-efficiency NL crystals. Recently four-photon entangled states have been generated with or without *quantum injection* [13–19]. Only very recently has been observed the generation of bipartite multiphoton entangled states created by means of HG SPDC been observed [20].

The aim of the present paper is to investigate theoretically and experimentally relevant aspects of the output wave function of SPDC in the HG regime. The adopted approach is to generate a multiphoton state and then to "extract" a two-photon component, which exhibits quite interesting features. This method, pioneered in [20], presents different advantages. First, the techniques for single-photon detection and characterization can be adopted. Second, it describes the loss effect associated with any communication process on a multiphoton entangled state.

Here we present a significant theoretical model to describe the overall process; then we provide a test of the model by a thorough experimental investigation. The propagation over a lossy channel is simulated by the conventional beam-splitter (BS) model. We analytically derive the density matrix of the two-photon state generated by postselection, after the effects of loss have taken place. On the theoretical side, the conceptually innovative contribution of the present work is the demonstration that the output state is a Werner state (WS) [21], i.e., a weighted superposition of a maximally entangled (singlet) state with a fully mixed state. Werner states play a paradigmatic role within quantum information; indeed they determine a family of mixed quantum states that includes both entangled and separable states. They model a decoherence process occurring on a singlet state traveling along a noisy channel, and hence are adopted to investigate the distillation and concentration processes [22–24]. Furthermore, depending on the singlet weight they can exhibit either entanglement and violation of Bell inequalities, or only entanglement, or separability.

The explicit dependence of the *singlet weight*, the characteristic parameter of the WS, on the NL gain value g of the SPDC has been theoretically derived leading to the demonstration that the two-photon state is entangled for any large value of g. The theory is supported by a thorough experimental investigation which shows the Werner feature of the output state. This condition is investigated thoroughly by exploiting the extensive knowledge available on Werner states, by modern techniques like the "entanglement witness," and by making connections with various forms of state entropy [25,26]. As a significant theoretical remark, note that while previous realizations of Werner states [26,27] were based on the realization of isotropic depolarizing channels acting on two-photon states, in the present context the Werner structure naturally arises as a consequence of the effect of the losses on the multiphoton state and of the subsequent projection of this state over a two-photon state.

The present paper is organized as follows. In Sec. II, the density matrix representing the two-photon reduced state arising from HG SPDC after propagation over lossy channels is analyzed theoretically. We find that, for any value of g, the resulting two-photon state is a Werner state. Resilience of entanglement is theoretically demonstrated for any value of g in the high-loss (HL) approximation. In Sec. III, the results of the theory are compared with the corresponding experimental data obtained by conventional quantum state tomography (QST) and by adopting entanglement-witness measurement procedures.

II. SPDC IN HIGH-LOSS REGIME: GENERATION OF WERNER STATES

In this section, we theoretically analyze the effect of losses on HG SPDC multiphoton states. Recently Durkin *et al.* [28] demonstrated the persistence of some kind of symmetry, implying entanglement in multiphoton SPDC states in the presence of polarization-independent photon losses. Here we explicitly derive the expression of the SPDC density matrix in the regime of induced high photon losses through coincidence measurements and demonstrate that it corresponds to a WS for any value of g. In the present model the effects of both losses and imperfect detections on the output states are simulated, as usual, by the insertion of beam splitters on the two propagation modes $\mathbf{k}_i$ ($i=1,2$) (Fig. 1). The results of this study demonstrate the resilience of bipartite entanglement for any value of g. This implies that, even in the absence of these induced losses, the initial SPDC state is entangled for any g, because of the basic impossibility of creating or enhancing the entanglement by means of local operations acting on a nonentangled state [29]. The main motivation for the present investigation resides in the experimental entanglement assessment on multiphoton HG fields by introducing light-absorbing filters on the correlated photon paths. The approximate expression of the density matrix also provides an intuitive explanation of the behavior of SPDC states in the HG and HL regimes.

The Hamiltonian of the SPDC process in the interaction picture reads [30,31]

$$\hat{H} = i\kappa(\hat{a}_{1H}^{\dagger}\hat{a}_{2V}^{\dagger} - \hat{a}_{1V}^{\dagger}\hat{a}_{2H}^{\dagger}) + \text{H.c.} \qquad (1)$$

where $\hat{a}_{ij}^{\dagger}$ represents the creation operators associated with the spatial propagation mode $\mathbf{k}_i$, with polarization $j=\{H,V\}$. H and V stand for horizontal and vertical polarization. κ is a coupling constant which depends on the crystal nonlinearity and is proportional to the amplitude of the pump beam. This Hamiltonian generates a unitary transformation $\hat{U}=e^{-i\hat{H}t/\hbar}$ acting on the input single-photon Fock state $|1\rangle_{1H}|0\rangle_{1V}|0\rangle_{2H}|0\rangle_{2V}=|1,0,0,0\rangle$. The output state $|\Psi^{out}\rangle = \hat{U}|1,0,0,0\rangle$ is easily obtained by virtue of the disentangling theorem [30,32,20]:

$$|\Psi^{out}\rangle = \frac{1}{C^2}\sum_{n=0}^{\infty}\sqrt{n+1}\,\Gamma^n|\psi_-^n\rangle \qquad (2)$$

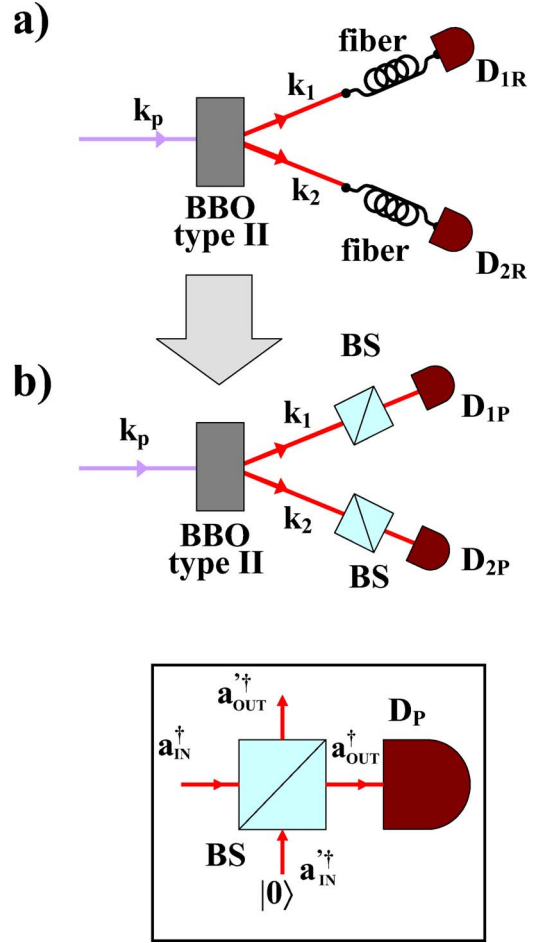where $|\psi_-^n\rangle$ is the n-generated pairs term:

FIG. 1. (Color online) (a) Schematic layout of the attenuated high-gain spontaneous parametric down-conversion generated in a type-II BBO nonlinear crystal. (b) Simulation of losses by the insertion of a beam splitter over each propagation mode k_i. Inset: each beam splitter couples input modes $a_{IN}^{\dagger}$, with unpopulated ones ($a_{IN}'^{\dagger}$).

$$|\psi_-^n\rangle = \frac{1}{\sqrt{n+1}}\sum_{m=0}^{n}(-1)^m|n-m\rangle_{1H}|m\rangle_{1V}|m\rangle_{2H}|n-m\rangle_{2V}$$

$$(3)$$

and $\Gamma=\tanh g$, $C=\cosh g$ [15]. The parameter $g\equiv\kappa t_{int}$ expresses the NL gain of the parametric process, t_{int} being the interaction time. The average number of photons generated per mode is equal to $\bar{n}=\sinh^2 g$.

Let us first consider the contribution $|\psi_-^n\rangle\langle\psi_-^n|$ to the overall density matrix. To investigate the propagation over a lossy channel, a beam splitter with transmittivity η for any polarization and spatial mode is assumed to simulate the effect of channel losses and of detector inefficiencies. Furthermore, perfect detectors with $\eta_{QE}=1$ measure the output state [33] (Fig. 1). The symmetry of the entangled state after losses is preserved by assuming η to be mode and polarization independent. The contribution $|\psi_-^n\rangle$ to the SPDC state is expressed in terms of the BS operators $\{\hat{a}_{ij\ in}^{\dagger}\}$ associated with the input modes $\{\mathbf{k}_i^{in}\}$:

$$|\psi_-^n\rangle = \frac{1}{\sqrt{n+1}} \frac{1}{n!} (\hat{a}_{1H\ in}^\dagger \hat{a}_{2V\ in}^\dagger - \hat{a}_{1V\ in}^\dagger \hat{a}_{2H\ in}^\dagger)^n |0,0,0,0\rangle. \quad (4)$$

The BS's couple the input modes $\{\mathbf{k}_i^{in}\}$ with the transmitted modes $\{\mathbf{k}_i^{out}\}$ and the reflected modes $\{\widetilde{\mathbf{k}}_i^{out}\}$. The output-state expression is found by substituting the operators $\{\hat{a}_{ij\ in}^\dagger\}$ with their expressions in term of the operators $\{\hat{a}_{ij\ out}^\dagger\}$, associated with the output transmitted modes $\{\mathbf{k}_i^{out}\}$, and the operators $\{\hat{b}_{ij\ out}^\dagger\}$, associated with the output reflected modes $\{\widetilde{\mathbf{k}}_i^{out}\}$, through the BS input-output matrix [33]

$$\begin{pmatrix} \hat{a}_{ij\ out}^\dagger(t) \\ \hat{b}_{ij\ out}^\dagger(t) \end{pmatrix} = \begin{pmatrix} \sqrt{\eta} & i\sqrt{1-\eta} \\ i\sqrt{1-\eta} & \sqrt{\eta} \end{pmatrix} \begin{pmatrix} \hat{a}_{ij\ in}^\dagger(t) \\ \hat{b}_{ij\ in}^\dagger(t) \end{pmatrix}. \quad (5)$$

The input state evolves into an output state which is defined over the four transmitted modes and the four reflected modes. This state is expressed through the Fock states $|n_{1H},n_{1V},n_{2H},n_{2V}\rangle_a \otimes |n_{1H},n_{1V},n_{2H},n_{2V}\rangle_b$ where the first term in the tensor product represents modes transmitted by the BS and hence detected ($\hat{a}$ modes) while the second term expresses the reflected modes ($\hat{b}$ modes).

The density matrix $\sigma^{out} = |\psi_-^n\rangle_{out}\langle\psi_-^n|_{out}$ of the n-pair term of the SPDC state can be easily obtained from the previous expressions:

$$\sigma^{out} = \frac{1}{n+1}\left(\frac{1}{n!}\right)^2 \sum_{k,l_i} \sum_{h,f_j} A^*(h,\{f_j\}) A(k,\{l_i\}) |l_1,l_2,l_3,l_4\rangle_a \otimes |n$$
$$-k-l_1,k-l_2,k-l_3,n-k-l_4\rangle_{ba}\langle f_1,f_2,f_3,f_4|\otimes_b\langle n-h$$
$$-f_1,h-f_2,h-f_3,n-h-f_4| \quad (6)$$

with

$$A(x,\{y_k\}) = \binom{n}{x}\binom{n-x}{y_1}\binom{x}{y_2}\binom{x}{y_3}\binom{n-x}{y_4}(-1)^x \eta^{y_1+y_2+y_3+y_4}(-i\sqrt{1-\eta})^{2n-y_1-y_2-y_3-y_4}$$
$$\times\sqrt{y_1!(n-x-y_1)!y_2!(x-y_2)!y_3!(x-y_3)!y_4!(n-x-y_4)!} \quad (7)$$

and $\Sigma_{x,y_i} \equiv \Sigma_{x=0}^n \Sigma_{y_1,y_4=0}^{n-x} \Sigma_{y_3,y_2=0}^x$. Since we are interested in the reduced density matrix ρ_a^n defined over the transmitted modes $\{\mathbf{k}_i^{out}\}$, $\rho_a^n = \mathrm{Tr}_b[|\psi_-^n\rangle\langle\psi_-^n|]^{out}$, we need to trace σ^{out} over the undetected reflected modes. The result is

$$\rho_a^n = \frac{1}{n+1}\left(\frac{1}{n!}\right)^2 \sum_{k,l_i} \sum_{h,f_j} A^*(h,\{f_j\}) A(k,\{l_i\})$$
$$\times |l_1,l_2,l_3,l_4\rangle_{aa}\langle f_1,f_2,f_3,f_4| \times \delta(n-k-l_1,n-h-f_1)$$
$$\times \delta(k-l_2,h-f_2)\delta(k-l_3,h-f_3)\delta(n-k-l_4,n-h-f_4). \quad (8)$$

The final expression for the n-pair contribution to the SPDC density matrix is

$$\rho_a^n = \frac{1}{n+1}\sum_{k,l_i}\sum_{h,f_j}(-1)^{k+h}(1-\eta)^{2n}S(h,k,l_2)S(h,k,l_3)$$
$$\times \widetilde{S}(h,k,l_1)\widetilde{S}(h,k,l_4)|l_1,l_2,l_3,l_4\rangle\langle k-h+l_1,h-k+l_2,h-k$$
$$+l_3,k-h+l_4| \quad (9)$$

where $S(h,k,p)=\zeta^p\sqrt{\binom{k}{p}\binom{h}{k-p}}$, $\widetilde{S}(h,k,p)=\zeta^p\sqrt{\binom{n-k}{p}\binom{n-h}{k-h+p}}$, and $\zeta = \frac{\eta}{1-\eta}$.

Up to now we have considered arbitrary, polarization-symmetric losses. In the following we make the additional assumption of very large losses, i.e., HL, which greatly simplifies our task. Such approximation is expressed by the re-lation $\eta\bar{n} \ll 1$, $\eta\bar{n}$ being the average number of photons transmitted by the BS per mode. This condition enables us to take into account only the terms of the sum Eq. (9) of order $\leqslant \eta^2$, hence considering only matrix elements corresponding to no more than two transmitted photons. As a final step, we assume to detect one photon on each mode $\mathbf{k}_i^{out}$ by the two-photon coincidence technique. In this way the vacuum terms affecting one or both vectors $\mathbf{k}_i^{out}$ are dropped. In summary, this coincidence procedure guarantees, by postselection, that we are dealing only with matrix elements arising from the tensor product of the states $\{|1,0,1,0\rangle, |1,0,0,1\rangle, |0,1,1,0\rangle, |0,1,0,1\rangle\}$, which correspond to the states $\{|H\rangle_1|H\rangle_2, |H\rangle_1|V\rangle_2, |V\rangle_1|H\rangle_2, |V\rangle_1|V\rangle_2\}$. The n-pair contribution ρ_{post}^n to the SPDC two-photon density matrix hence reads

$$\rho_{post}^n = \frac{1}{6}n(1-\eta)^{2n}$$
$$\times \zeta^2 \begin{pmatrix} (n-1) & 0 & 0 & 0 \\ 0 & (1+2n) & -(n+2) & 0 \\ 0 & -(n+2) & (1+2n) & 0 \\ 0 & 0 & 0 & (n-1) \end{pmatrix}. \quad (10)$$

We note that the above density matrix has the form of a Werner state $\rho_W = p|\Psi_-\rangle\langle\Psi_-| + \frac{1-p}{4}I$, with $p=\frac{(n+2)}{3n}$, which is a mixture with probability p of the maximally entangled state
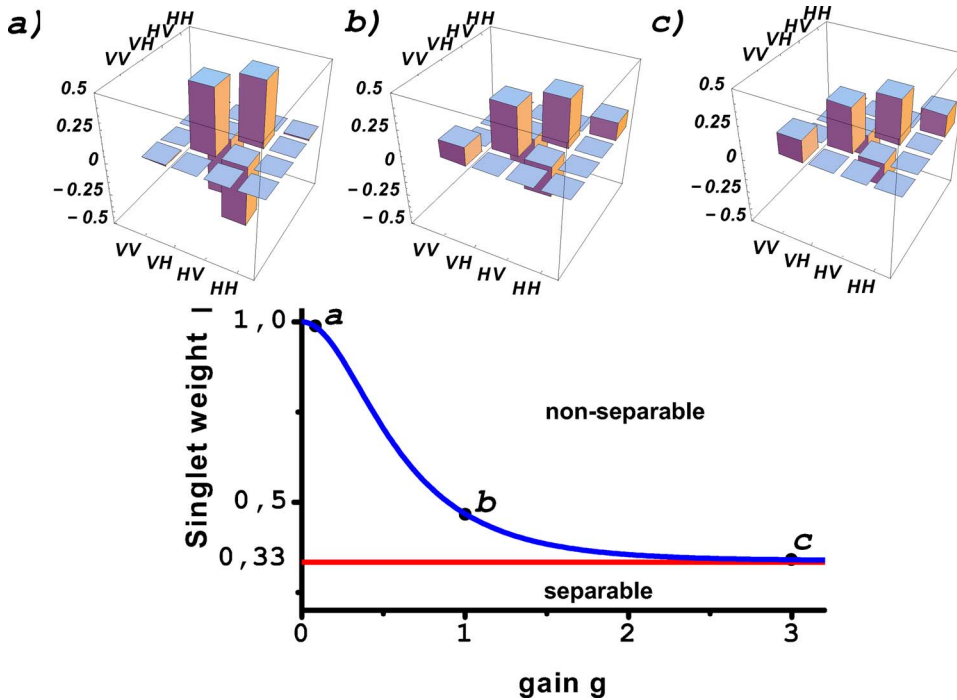
FIG. 2. (Color online) Theoretical singlet weight p of the Werner states versus nonlinear parametric gain g. The theoretical two-photon density matrices ρ_{th}^{II} are reported for some gain values ($g = 0.1, 1, 3$).

$|\Psi_-\rangle = 2^{-1/2}(|H\rangle_1|V\rangle_2 - |V\rangle_1|H\rangle_2)$ and of the maximally chaotic state $I/4$, I being the identity operator on the overall Hilbert space. These states are commonly adopted in QI, since they model a decoherence process occurring on a singlet state traveling along an isotropic noisy channel [34].

The complete density matrix for the SPDC output state is obtained by substituting the ρ_{post}^n matrices into the expression $\rho_{th}^{II} = \frac{1}{C^4}\sum_{n=0}^{\infty}(n+1)\Gamma^{2n}\rho_{post}^n$. All the terms ρ_{post}^n sum up incoherently. Let us explain the latter procedure. In the actual conditions any $[|\psi_-^n\rangle\langle\psi_-^n|]$ leads, after the BS action, to two transmitted photons and $2(n-1)$ reflected photons. Different n numbers of input pairs lead to the discard of different numbers of reflected photons; hence any mutual coherence is destroyed after the tracing operation. The normalized density matrix turns out to be

$$\rho_{th}^{II} = \begin{pmatrix} \frac{1-p}{4} & 0 & 0 & 0 \\ 0 & \frac{1+p}{4} & -\frac{p}{2} & 0 \\ 0 & -\frac{p}{2} & \frac{1+p}{4} & 0 \\ 0 & 0 & 0 & \frac{1-p}{4} \end{pmatrix}. \quad (11)$$

The SPDC density matrix ρ_{th}^{II}, given by the sum of Werner states, is a WS itself, with singlet weight

$$p = \frac{1}{2\tilde{\Gamma}^2 + 1} \quad (12)$$

with $\tilde{\Gamma} = (1 - \eta)\tanh g$. In the limit $\eta \to 0$, $\tilde{\Gamma} = \tanh g$. For large values of g, i.e., for $\tilde{\Gamma} \to 1$, and in the hypothesis of very high

losses, the singlet weight $p \geqslant \frac{1}{3}$ approaches the minimum value $\frac{1}{3}$. Since the condition $p > \frac{1}{3}$ implies the well-known nonseparability condition for a general WS, we have demonstrated for large g the expected high resilience against decoherence of the entangled singlet state [21]. The graph of Fig. 2 shows the behavior of singlet weight p as a function of the interaction parameter g.

III. EXPERIMENTAL REALIZATION

The previous theoretical results have been experimentally tested for different values of the parametric NL gain g (Fig. 3). The main source was a Ti:sapphire mode-locked laser (device Coherent MIRA) further amplified by a Ti:sapphire regenerative amplifier (Coherent Rega 9000) (A) operating with pulse duration 180 fs. The amplifier could operate at a repetition rate either 250 or 100 kHz leading to an energy per pulse, respectively, of 4 and 8 μJ. The output beam was frequency doubled in a uv beam at $\lambda_p = 397.5$ nm through a second harmonic generation (SHG) process, achieved by focusing the infrared beam into a 1-mm-thick β–barium borate (BBO) crystal, cut for type-I phase matching, through a lens with focal length of 20 cm. The nonlinear crystal was placed at 5 cm from the beam waist in order to avoid crystal damage and beam spatial distortion. The uv beam then excited a SPDC process in an $L = 1.5$-mm-thick BBO NL crystal slab (Fig. 3). The SPDC-generated photons with degenerate wavelengths (WL's) $\lambda = 2\lambda_p = 795$ nm propagated along the $\mathbf{k}_1$ and $\mathbf{k}_2$ modes. A $\lambda/2$ wave plate (WP) and an $\frac{L}{2}$ thick BBO crystal were placed on each mode to ensure the accurate compensation of all residual birefringence effects coming from the main BBO crystal, cut for type-II phase matching [5]. In each mode $\mathbf{k}_i$, an additional glass plate (G_p) ensured a tight balance between the two polarization emission cones of the SPDC process. The balance between the
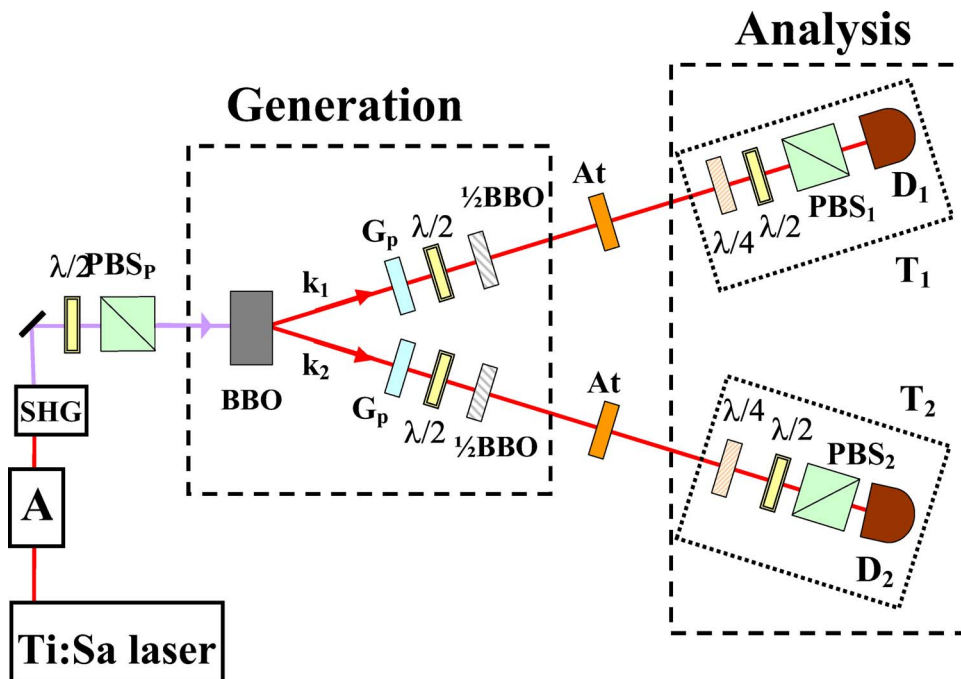
Generation

Analysis

FIG. 3. (Color online) Experimental setup adopted for multiphoton-state generation by means of SPDC process and characterization by QST (tomographic setups T_i).

two cones was achieved by suitable tilting of G_p in order to vary the ratio between the transmittivities for the s- and p-polarized waves. Calibrated neutral attenuation filters (At) placed along modes $\mathbf{k}_1$ and $\mathbf{k}_2$ were adopted to assure the condition of high losses and hence the single-photon detection regime. The polarization-state analysis was carried out through two π analyzers (T_1 and T_2 in Fig. 3) each one consisting of a pair of $\lambda/4 + \lambda/2$ optical wave plates, a polarizing beam splitter (PBS), a single-mode fiber-coupled detector *SPCM-AQR*14-*FC* with an interferential filter of bandwidth $\Delta\lambda = 4.5$ nm placed in front of it. The combination of the uv $\lambda/2$ WP (WP$_P$) and PBS$_P$ allowed a fine tuning of the uv pump power exciting the NL crystal.

In a first experiment we estimated the gain value g of the optical parametric process and the overall quantum efficiencies of the detection apparatus on both modes. The count rates of D_1 and D_2 and the coincidence rate of $[D_1, D_2]$ were measured for different values of the uv power (Fig. 4). The plots of Figs. 4(a) and 4(b) clearly show the onset of the NL parametric interaction with large g, thus implying the generation of many photon pairs. The gain value of the process is obtained by fitting the count rates N_i of detector D_i, depending on the uv pump power P_{uv}, with the function $N_i(g) = R \frac{\eta_i \Gamma^2}{1-(1-\eta_i)\Gamma^2}$ [20] where $\Gamma = \tanh g$ η_i is the quantum efficiency on mode $\mathbf{k}_i$, and R is the repetition rate of the pump source. The gain value g depends on the uv power, namely, $g = \gamma\sqrt{P_{uv}}$, where the parameter γ takes into account the efficiency of the NL process. The maximal value of gain obtained has been found as $g_{max} = 1.39 \pm 0.05$, which leads to a mean photon number per mode $\bar{n} = \sinh^2 g_{max} = 3.5 \pm 0.4$. In conclusion the maximal total number of generated photons on $\mathbf{k}_1$ and $\mathbf{k}_2$ modes through the SPDC process is $M = 4\bar{n} = 14.0 \pm 1.6$. By means of the previous fits, we could also estimate the overall detection efficiencies η_i on the $\mathbf{k}_i$ mode, which results from the glass attenuation, the fiber coupling, and the detection quantum efficiencies: $\eta_1 = 0.036 \pm 0.005$

and $\eta_2 = 0.037 \pm 0.005$. Using the previous values we find $\eta\bar{n} \simeq 0.1$. The detected coincidence rate N_{12} of $[D_1, D_2]$ is easily found to be described by the following expression:

$$N_{12}(g) = R \frac{\eta_1 \eta_2 \Gamma^2 (\Gamma^4 t_1 t_2 - 1)}{(1 - \Gamma^2 t_1)(1 - \Gamma^2 t_2)(\Gamma^2 t_1 t_2 - 1)} \quad (13)$$

with $t_i = 1 - \eta_i$. Figure 4(b) reports the measured rate coincidence and the fit curve with the model of Eq. (13). Starting from the previous values of η_i, by the last fit we obtained $\tilde{g}_{max} = 1.334 \pm 0.001$. This value is found slightly lower than
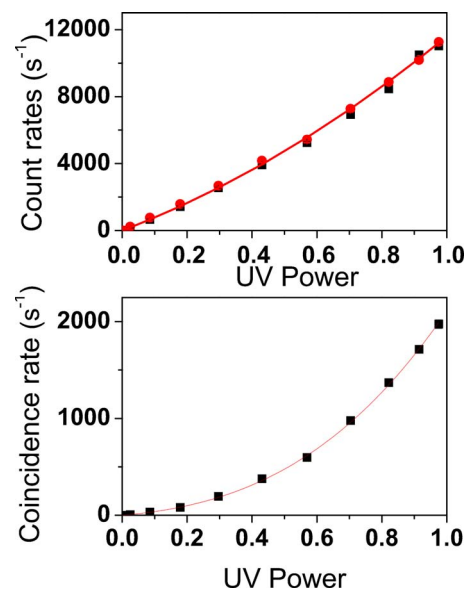

FIG. 4. (Color online) (a) Count rates of $[D_1]$ and $[D_2]$ as a function of the normalized uv power. The continuous line expresses the best-fit result. (b) Coincidence rate of $[D_1, D_2]$ as a function of the normalized uv power. The continuous line expresses the best-fit result.
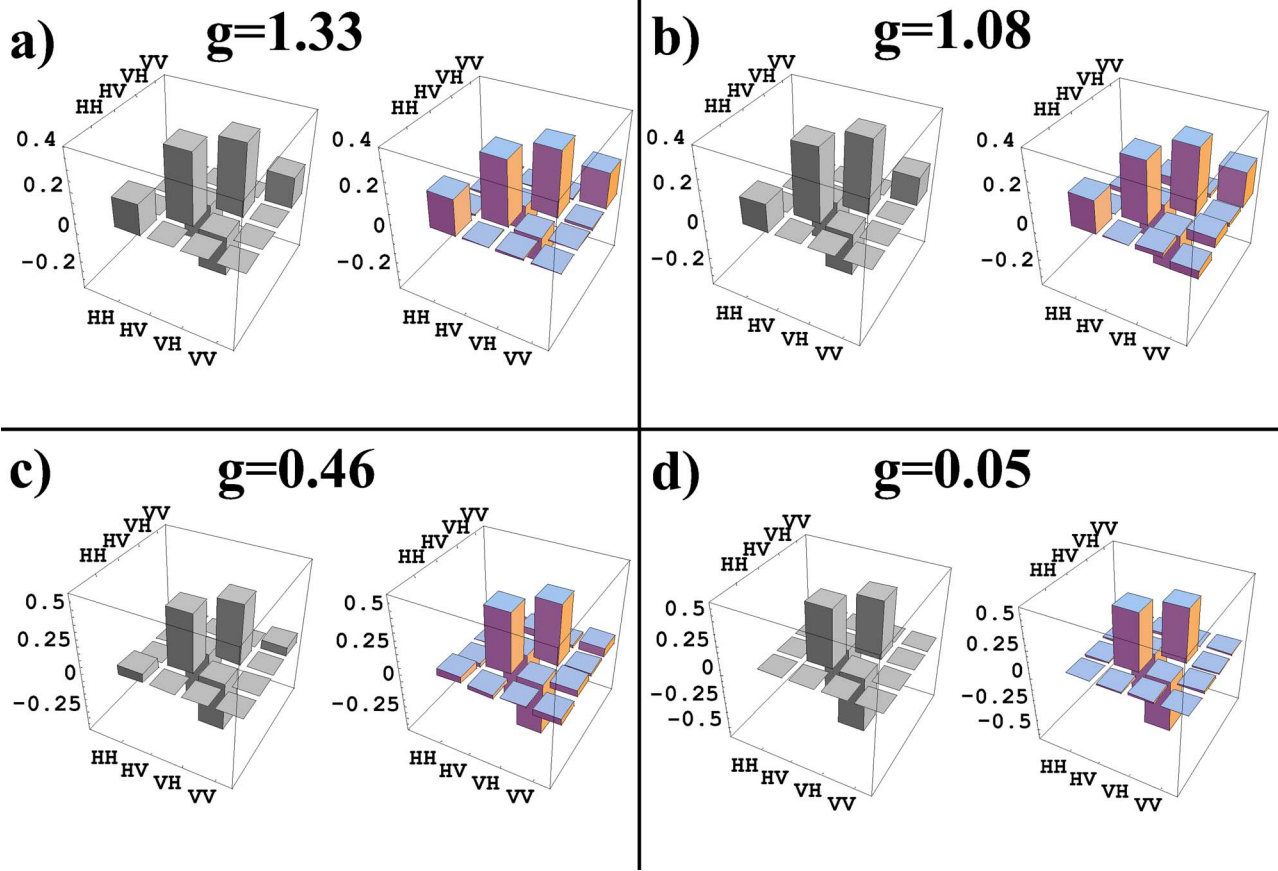
FIG. 5. (Color online) Theoretical ρ_{th} (left plot) and experimental ρ_{expt}^{II} (right plot) density matrices for different gain values g. The experimental density matrices have been reconstructed by measuring 16 two-qubit observables through the two tomographic setups $\{T_i\}$. Each tomographic measurement lasted a time t and yielded maximum twofold counts (CC) for the $|HV\rangle$ projection of (a) $t=1$ s, CC $\simeq 9300$; (b) $t=2$ s, CC $\simeq 12\,000$; (c) $t=15$ s, CC $\simeq 2000$; (d) $t=120$ s, CC $\simeq 1300$.

the value of g_{max}. This discrepancy can be attributed to an imperfect spatial correlation between the two fiber-coupled modes $\mathbf{k}_1$ and $\mathbf{k}_2$, which causes a decrease in the coincidence rate.

The main experimental result of the present work is the full characterization of the two-photon state. We reconstructed the density matrix ρ_{expt}^{II} of the generated two-qubit state on $\mathbf{k}_1$ and $\mathbf{k}_2$ modes by adopting the quantum state tomography method [35]. The experimental density matrix ρ_{expt}^{II} is obtained by first measuring the two-photon coincidences $[D_1, D_2]$ for different settings of the QST setup, T_1 and T_2, and then by applying a numerical algorithm to estimate the density matrix. In a low-gain condition the SPDC state generated on $\mathbf{k}_1$ and $\mathbf{k}_2$ modes is expected to be in the singlet state $|\Psi^-\rangle = 2^{-1/2}(|H\rangle_{k_1}|V\rangle_{k_2} - |V\rangle_{k_1}|H\rangle_{k_2})$, with excellent agreement between theory and experiment [Fig. 5(d)]. By increasing g, the ρ elements corresponding to $|H\rangle_{k_1}|H\rangle_{k_2 k_1}\langle H|_{k_2}\langle H|$ and $|V\rangle_{k_1}|V\rangle_{k_2 k_1}\langle V|_{k_2}\langle V|$ are no longer negligible and the detection of two photons with the same polarization is a consequence of the multipair condition [Figs. 5(a)–5(c)]. The experimental results for the density matrices ρ_{expt}^{II} for different g values are in good agreement with the theoretical prediction ρ_{th}^{II}; the mean value of fidelity

between the four comparisons is $\mathcal{F} = 0.996 \pm 0.002$, where

$$\mathcal{F}(\rho_{th}^{II}, \rho_{expt}^{II}) = \mathrm{Tr}^2 \sqrt{\sqrt{\rho_{th}^{II}} \rho_{expt}^{II} \sqrt{\rho_{th}^{II}}}.$$

The density matrices ρ_{expt}^{II} can now be adopted to estimate the *singlet weight, tangle*, and *linear entropy* of the generated state. The density matrix ρ_W of a Werner state is given by the expression (11), as said. The singlet weight (p) can be directly obtained from the matrix elements as $p = (\rho_{expt}^{II})_{22} + (\rho_{expt}^{II})_{33} - (\rho_{expt}^{II})_{11} - (\rho_{expt}^{II})_{44}$. Werner states are entangled ($p > \frac{1}{3}$) or separable ($p \leq \frac{1}{3}$), the extreme conditions being the pure singlet ($p=1$) and the totally mixed state ($p=0$). The tangle is a parameter expressing the degree of entanglement of the state, which is defined as $\tau = C^2$, where C is the concurrence of the state [36]; $\tau > 0$ is a necessary and sufficient condition for a 2×2 state to be entangled. Another important property for a mixed state is *linear entropy* (S), which quantifies the degree of disorder, viz., the mixedeness of the system. For a system of dimension 4, it is given by $S = \frac{4}{3}[1 - \mathrm{Tr}(\rho^2)]$. In the case of a Werner state, we have $S_W = (1 - p^2)$. For Werner states, tangle and linear entropy are found to be related as follows [37,38]:
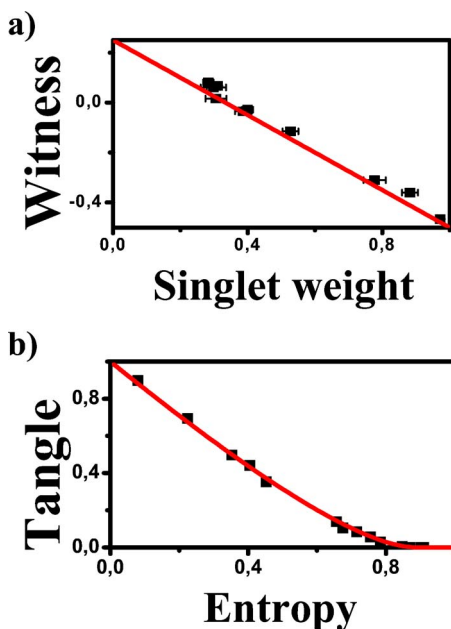
FIG. 6. (Color online) (a) Measured tangle parameter τ as a function of the entropy S of the state. Continuous line, theoretical plot (14). (b) Measured witness parameter $W = \mathrm{Tr}(\hat{O}_W \rho_{expt}^{II})$ as a function of singlet weight p. Continuous line, theoretical plot (16).

$$\tau(S_W) = \begin{cases} \dfrac{1}{4}(1 - 3\sqrt{1 - S_W})^2 & \text{for } 0 \leqslant S_W \leqslant \dfrac{8}{9}, \\ 0 & \text{for } \dfrac{8}{9} \leqslant S_W \leqslant 1. \end{cases} \quad (14)$$

For each experimental value of g, (S, τ) are estimated starting from the experimental density matrix. The agreement between experimental results and theoretical predictions is found satisfactory [Fig. 6(a)].

An alternative method to establish whether a state is entangled or not is based on the concept of entanglement witness. The estimation of the tangle adopted above requires the complete knowledge of the density matrix of the bipartite quantum system. On the other hand, the entanglement witness exploits partial *a priori* knowledge of the quantum state, in particular the class to which it belongs: here the Werner one. It can be directly estimated with fewer measurements (in the present case 9 instead of 16) and with a simpler data elaboration. A state ρ is entangled if and only if there exists a Hermitian operator $\hat{O}$, a so-called entanglement witness, which has positive expectation value $\mathrm{Tr}(\hat{O}\rho_{sep}) \geqslant 0$ for all separable states ρ_{sep} and has negative expectation value $\mathrm{Tr}(\hat{O}\rho) < 0$ on the state ρ [39–43]. For Werner states ρ_W the method proposed in [25,44] leads to the following entanglement-witness operator:

$$\hat{O}_W = \frac{1}{2}(|H\rangle|H\rangle\langle H|\langle H| + |V\rangle|V\rangle\langle V|\langle V| + |D\rangle|D\rangle\langle D|\langle D|$$

$$+ |F\rangle|F\rangle\langle F|\langle F| - |L\rangle|R\rangle\langle L|\langle R| - |R\rangle|L\rangle\langle R|\langle L|) \quad (15)$$

where $|D\rangle = \frac{1}{\sqrt{2}}(|H\rangle + |V\rangle)$ and $|F\rangle = \frac{1}{\sqrt{2}}(|H\rangle - |V\rangle)$ express diagonally polarized single-photon states, while $|L\rangle = \frac{1}{\sqrt{2}}(|H\rangle + i|V\rangle)$ and $|R\rangle = \frac{1}{\sqrt{2}}(|H\rangle - i|V\rangle)$ express left- and right-circular polarization states. The relationship between the expectation value for a Werner state $W_W = \mathrm{Tr}(\hat{O}_W \rho_W)$ and the Werner weight p is found to be

$$W_W(p) = \frac{1 - 3p}{4} \quad (16)$$

[7], leading to $W_W(p) < 0$ for $p > \frac{1}{3}$. Experimentally $\mathrm{Tr}(\hat{O}_W \rho_{expt}^{II})$ has been estimated through eight projective measurements (the six projectors appearing in (15) and the operators $\{|H\rangle|V\rangle\langle H|\langle V|, |V\rangle|H\rangle\langle V|\langle H|\}$ for normalization [26]). In conclusion, for each g value, a point of the Cartesian plane of coordinates (p, W) is obtained [Fig. 6(b)]. The solid line reports the theoretical dependence (16). The comparison demonstrates a good agreement between the theoretical prediction and experimental results.

By the different methods described above the entanglement condition has been found to be realized for a value of g up to 1.15 ± 0.02 [Fig. 5(c)], corresponding to an average number of photons equal to $M = 4\bar{n} = 8.0 \pm 0.8$ before losses. For higher values of g the presence of bipartite entanglement is degraded by decoherence effects, mostly due to imperfect correction of the walk-off effect in the BBO crystal and to time distinguishability introduced by the femtosecond pump pulse.

IV. CONCLUSIONS

In summary, the present work shows that the multiphoton states generated by SPDC exhibit a bipartite entanglement even in the presence of high losses, confirming previous analysis [28]. An explicit form has been derived for the output two-photon state: a Werner state. The theoretical results are found to be in very good agreement with experimental data. We believe that the present results could be useful to investigate the resilience of entanglement in lossy communication. The present approach can be extended to investigate the quantum injected optical parametric amplifier [45,15,16].

[1] R. Raussendorf and H. J. Briegel, Phys. Rev. Lett. **86**, 5188 (2001); P. Walther *et al.*, Nature (London) **434**, 169 (2005).

[2] A. N. Boto *et al.*, Phys. Rev. Lett. **85**, 2733 (2000).

[3] D. Bouwmeester *et al.*, Nature (London) **390**, 575 (1997); D. Boschi, S. Branca, F. De Martini, L. Hardy, and S. Popescu, Phys. Rev. Lett. **80**, 1121 (1998); E. Lombardi, F. Sciarrino, S. Popescu, and F. De Martini, *ibid.* **88**, 070402 (2002).

[4] N. Gisin, G. Ribordy, W. Tittel, and H. Zbinden, Rev. Mod. Phys. **74**, 145 (2002).

[5] P. G. Kwiat, K. Mattle, H. Weinfurter, A. Zeilinger, A. V. Sergienko, and Y. Shih, Phys. Rev. Lett. **75**, 4337 (1995).

[6] P. G. Kwiat, E. Waks, A. G. White, I. Appelbaum, and P. H. Eberhard, Phys. Rev. A **60**, R773 (1999).

[7] C. Cinelli, G. Di Nepi, F. De Martini, M. Barbieri, and P. Mataloni, Phys. Rev. A **70**, 022321 (2004).

[8] M. Fiorentino, G. Messin, C. E. Kuklewicz, F. N. C. Wong, and J. H. Shapiro, Phys. Rev. A **69**, 041801 (2004).

[9] C. Kurtsiefer, M. Oberparleiter, and H. Weinfurter, Phys. Rev. A **64**, 023802(R) (2001).

[10] G. A. Durkin, C. Simon, and D. Bouwmeester, Phys. Rev. Lett. **88**, 187902 (2002).

[11] M. D. Reid, W. J. Munro, and F. De Martini, Phys. Rev. A **66**, 033801 (2002).

[12] C. Simon and D. Bouwmeester, Phys. Rev. Lett. **91**, 053601 (2003).

[13] F. De Martini, V. Mussi, and G. Di Giuseppe, Opt. Commun. **179**, 581 (2000); F. De Martini, G. Di Giuseppe, and S. Padua, Phys. Rev. Lett. **87**, 150401 (2001).

[14] A. Lamas-Linares, J. C. Howell, and D. Bouwmeester, Nature (London) **412**, 887 (2001); J. C. Howell, A. Lamas-Linares, and D. Bouwmeester, Phys. Rev. Lett. **88**, 030401 (2002).

[15] D. Pelliccia, V. Schettini, F. Sciarrino, C. Sias, and F. De Martini, Phys. Rev. A **68**, 042306 (2003).

[16] F. De Martini, D. Pelliccia, and F. Sciarrino, Phys. Rev. Lett. **92**, 067901 (2004).

[17] M. Eibl *et al.*, Phys. Rev. Lett. **90**, 200403 (2003).

[18] Z. Zhao *et al.*, Nature (London) **430**, 54 (2004).

[19] F. De Martini, F. Sciarrino, and V. Secondi, Phys. Rev. Lett. **95**, 240401 (2005).

[20] H. S. Eisenberg, G. Khoury, G. Durkin, C. Simon, and D. Bouwmeester, Phys. Rev. Lett. **93**, 193901 (2004).

[21] R. F. Werner, Phys. Rev. A **40**, 4277 (1989).

[22] T.-C. Wei *et al.*, Phys. Rev. A **71**, 032329 (2005).

[23] A. Sen(De), U. Sen, C. Brukner, V. Buzek, and M. Zukowski, Phys. Rev. A **72**, 042310 (2005).

[24] M. S. Anwar *et al.*, Phys. Rev. A **71**, 032327 (2005).

[25] O. Gühne *et al.*, Phys. Rev. A **66**, 062305 (2002).

[26] M. Barbieri, F. De Martini, G. Di Nepi, P. Mataloni, G. M. D'Ariano, and C. Macciavello, Phys. Rev. Lett. **91**, 227901 (2003).

[27] J. B. Altepeter *et al.*, Phys. Rev. Lett. **90**, 193601 (2003).

[28] G. A. Durkin, C. Simon, J. Eisert, and D. Bouwmeester, Phys. Rev. A **70**, 062305 (2004).

[29] V. Vedral and M. B. Plenio, Phys. Rev. A **57**, 1619 (1998).

[30] F. De Martini, Phys. Rev. Lett. **81**, 2842 (1998).

[31] F. De Martini and F. Sciarrino, Prog. Quantum Electron. **29**, 165 (2005).

[32] M. J. Collet, Phys. Rev. A **38**, 2233 (1988).

[33] R. Loudon, *The Quantum Theory of Light*, 3rd ed. (Oxford University Press, New York, 2000), Secs. 5.7 and 6.10.

[34] M. A. Nielsen and I. L. Chuang, *Quantum Computation and Quantum Information* (Cambridge University, Cambridge, U.K., 2000).

[35] D. F. V. James, P. G. Kwiat, W. J. Munro, and A. G. White, Phys. Rev. A **64**, 052312 (2001).

[36] T. Wei *et al.*, Phys. Rev. A **67**, 022110 (2003).

[37] W. J. Munro, D. F. V. James, A. G. White, and P. G. Kwiat, Phys. Rev. A **64**, 030302 (2001).

[38] M. Barbieri, F. De Martini, G. Di Nepi, and P. Mataloni, Phys. Rev. Lett. **92**, 177901 (2004).

[39] M. Horodecki, P. Horodecki, and R. Horodecki, Phys. Lett. A **223**, 1 (1996).

[40] B. Terhal, Phys. Lett. A **271**, 319 (2000).

[41] M. Lewenstein, B. Kraus, J. I. Cirac, and P. Horodecki, Phys. Rev. A **62**, 052310 (2000).

[42] M. Lewenstein, B. Kraus, P. Horodecki, and J. I. Cirac, Phys. Rev. A **63**, 044304 (2001).

[43] D. Bruß *et al.*, J. Mod. Opt. **49**, 1399 (2002).

[44] G. M. D'Ariano, C. Macchiavello, and M. G. A. Paris, Phys. Rev. A **67**, 042310 (2003).

[45] F. De Martini, V. Bužek, F. Sciarrino, and C. Sias, Nature (London) **419**, 815 (2002).